Relaxometric and solution NMR structural studies on ditopic lanthanide(III) complexes of a phosphinate analogue of DOTA with a fast rate of water exchange†

Jakub Rudovský,[a] Mauro Botta,*[b] Petr Hermann,*[a] Avtandil Koridze[c] and Silvio Aime[d]

Received 21st December 2005, Accepted 17th March 2006
First published as an Advance Article on the web 29th March 2006
DOI: 10.1039/b518147j

A novel "ditopic" ligand containing two monophosphinate triacetate DOTA-like units linked by a thiourea bridge has been synthesized and its complexes with Ln^{3+} ions (Ln = Y, Eu, Gd, Dy) investigated by NMR spectroscopy and relaxometry. The presence of one water molecule in the first coordination sphere has been determined by the measurement of the dysprosium(III)-induced ^{17}O NMR shifts. The ^{1}H and ^{31}P NMR spectra of the Eu^{III} derivative indicate a higher abundance of the fast-exchanging twisted square antiprismatic (***m***) isomer than the isomeric square antiprismatic (***M***; ***m***/***M*** = 3 : 2) complex. The analysis of the ^{89}Y and ^{13}C T_1 NMR relaxation times in the Gd^{III}/Y^{III} mixed complex have provided useful structural information. Values of *ca.* 6.3 and 8.2 Å for the Gd ··· Y and Gd ··· C distances, respectively, have been estimated which indicate a rather compact solution structure. This result finds support in the value of the relaxivity whose increase (at 20 MHz and 298 K) on passing from the monomeric (5.7 s^{-1} mM^{-1}) to the ditopic complex (8.2 s^{-1} mM^{-1}) can be attributed to the doubling of the inner-sphere term following the doubling of the molecular size. The structural and dynamic relaxivity-controlling parameters were assessed by a simultaneous fitting of the variable temperature ^{17}O NMR and ^{1}H NMRD relaxometric data. The mean water residence lifetime ($^{298}\tau_M$) has been found to be 53 ns, one of the shortest values reported for ditopic complexes. The reorientational correlation time is two times longer ($^{298}\tau_R$ = 183 ps) than the corresponding value of the parent monomeric Gd^{III} complex, thus supporting the view of a limited degree of internal rotation. The possible influence of magnetic Gd–Gd coupling has been excluded by a comparison of the ^{1}H NMRD profiles of the homodinuclear Gd^{III}/Gd^{III} and the heterodinuclear Gd^{III}/Y^{III} complexes.

Introduction

During the last two decades, magnetic resonance imaging (MRI) has became one of the most powerful diagnostic methods in medicine. It has been proved to be particularly suitable for the imaging of soft tissues with an excellent spatial resolution. The intrinsic contrast of MRI images originates from local variation in concentration and nuclear magnetic relaxation times of water protons. This contrast is further enhanced by the administration of paramagnetic contrast agents (CA). These compounds function by catalyzing the proton magnetic relaxation times of nearby water protons in the tissues where they are distributed, thus increasing the contrast between healthy and pathological regions. Nowadays, more than 30% of the MRI investigations make use of CA. The most common class of T_1–CA is represented by the complexes of the highly paramagnetic Gd^{3+} ion, where the central ion is encapsulated in an organic ligand leaving just one or two coordination sites available for water molecule(s). It is the chemical exchange of the coordinated water molecule(s) with the bulk water that transfers the paramagnetic relaxation to the surrounding tissues giving rise to the contrast enhancement.

The extensive investigations carried out in the last 10–15 years have provided chemists with a good understanding of the relationship between the structural properties of the Gd^{III} complex and the *relaxivity* (r_1). This is a parameter that measures the efficacy of a metal-based CA and is defined as the increase in the ^{1}H relaxation rate of water protons in the presence of a 1 mM concentration of the paramagnetic complex.[1–4] The relaxivity values predicted by theoretical models of paramagnetic relaxation are much higher ($\geq$100 s^{-1} mM^{-1}) than those typical of the commercial CA (*ca.* 4–5 s^{-1} mM^{-1}).[5] It is also well known that, in order to attain the high relaxivity values required by the new, emerging applications of MRI, *e.g.* in molecular imaging,[6–8] several structural and dynamic parameters of the gadolinium(III) chelates need to be optimized. The most important factors

[a]*Department of Inorganic Chemistry, Charles University, Hlavova 2030, 128 40, Prague 2, Czech Republic. E-mail: petrh@natur.cuni.cz; Fax: +420 22195-1253; Tel: +420 22195-1263*
[b]*Department of Environmental and Life Sciences, University of Eastern Piedmont "A. Avogadro", Via Bellini 25/G, I-15100, Alessandria, Italy. E-mail: mauro.botta@mfn.unipmn.it; Fax: +39 0131-360250; Tel: +39 0131-360253*
[c]*Department of Chemistry, I. Javakhishvili Tbilisi State University, 3 Chavchavadze ave., 380028, Tbilisi, Georgia*
[d]*Department of Chemistry I. F. M., University of Torino, Via P. Giuria 7, I-10125, Torino, Italy*

† Electronic supplementary information (ESI) available: Fig. S1: $GdCl_3$ relaxometric titration of the title ligand. Fig. S2: Dy^{III}-induced ^{17}O chemical shift measurement. Fig. S3: ^{1}H NMR spectrum of the Eu^{III}–Eu^{III} complex. Fig. S4: Dependence of ^{1}H relaxivity on pH. Fig. S5: ^{13}C NMR spectra of the free ligand and its Gd^{III}–Y^{III} complex. Table S1: The complete set of all possible isomers of the dinuclear complexes. Table S2: ^{13}C relaxation times of the Gd^{III}–Y^{III} complex. Full set of SBM and SC equations used for fitting of relaxometric data. See DOI: 10.1039/b518147j

are certainly the residence lifetime of the coordinated water molecule(s), τ_M, the rotational correlation time of the Gd–H_w vector, τ_R, and the electron-spin relaxation parameters. Ideally, a Gd^{III} complex should reorient in solution at a rate of the order of $\approx 10^9$ s^{-1}, possess a coordinated water molecule exchanging at a rate ($k_{ex} = 1/\tau_M$) of $\approx 10^8$ s^{-1}, and be characterized by electronic relaxation times as long as possible. Different strategies have been devised in order to accelerate the slow water exchange rate of the commercial CA and obtain gadolinium(III) chelates with τ_M values in the optimal range.[9–15] Recently, we have demonstrated that the introduction of a phosphorous acid moiety into a DOTA-like macrocyclic ligand structure (H_4DOTA = 1,4,7,10-tetraazacyclododecane-1,4,7,10-tetracetic acid; Chart 1) induces a pronounced increase in the rate of water exchange in the corresponding gadolinium(III) chelate.[12–14] Furthermore, the replacement of a carboxylate with a phosphorous acid group favours the formation of hydrogen-bonded, second-sphere water molecules that contribute to the relaxivity of the Gd^{III} complex,[16] and allows for bifunctionality that is essential for further covalent conjugation. These properties have been recently exploited for the preparation of high relaxivity PAMAM [poly(amido amine)] conjugates with monophosphinate DOTA-like units, DO3A-P^{ABn} (H_4DO3A-P^{ABn} = 1,4,7,10-tetraazacyclododecane-4,7,10-triacetic-1-{methyl[(4-aminophenyl)methyl)]phosphinic acid}; Chart 1).[17]

The fast molecular reorientation of the commercial CA in solution is responsible of their low relaxivity values at the imaging fields. Clearly, every attempt at enhancing the relaxivity needs to be focused primarily on the increase of τ_R either by increasing the size of the complexes or by attaching the complexes to macromolecular substrates. A relatively simple strategy is the preparation of dimeric or multimeric metal chelates. However, up to now, only few examples of this class of Gd^{III} complex have been reported, based on the DTPA- or DOTA-like basic structures. The most investigated compounds have been the dinuclear[18–22] and multinuclear[23] complexes of mostly amide derivatives of DOTA characterized by a rather slow rate of water exchange. Only very recently, a few nice examples of multimeric complexes exhibiting a high relaxivity due to the presence of two coordinated water molecules have been investigated.[24] Unfortunately, these complexes are rather thermodynamically and kinetically unstable due to either the relatively low number of donor atoms or the open-chain structure of the ligand.

In this paper, we present a detailed NMR and relaxometric study of lanthanide(III) complexes with a new ditopic ligand (Chart 1) of general formula $[Ln_2(CS(DO3A\text{-}P^{NBn})_2)(H_2O)_2]^{2-}$. The two monomeric units are connected by a thiourea moiety commonly used for the conjugation of small ligands to biomolecules.[25] Because of the favourable properties of the parent monomeric Gd-DO3A-P^{ABn} complex, the related novel ditopic complex is expected to have a high thermodynamic and kinetic stability in addition to exchanging water rapidly.

Results and discussion

Synthesis and characterization

The desired ligand was first isolated as a byproduct from the conjugation reaction used in the preparation of the PAMAM dendrimeric conjugates with the corresponding monomeric DO3A-P^{ABn} ligand.[17] It is worth noting that a "dimerization" reaction of this type invariably takes place during the conjugation of isothiocyanates to any amine (*e.g.* PAMAM dendrimers) as a side-reaction. The isothiocyanate group undergoes a hydrolysis to the parent amine even under mild basic conditions (pH 8–9). The amine subsequently reacts with the isothiocyanate group of another molecule to produce the symmetrical dimeric structure through the thiourea bridge. Bearing this in mind, we set up a controlled coupling reaction between the amine (DO3A-P^{ABn}) and its corresponding isothiocyanate derivative (DO3A-P^{NCS}; Chart 1) in order to prepare larger amounts of the ditopic ligand CS(DO3A-P^{NBn})$_2$. Both components were mixed in water and the pH was adjusted to 9–10 with 2 M KOH. The mixture was then stirred at room temperature and the course of the reaction was monitored by TLC until the monomeric component disappeared (8 hours). The crude product was then purified by chromatography on Amberlite CG50 cation-exchange resin in H^+-cycle. The desired CS(DO3A-P^{NBn})$_2$ ligand was finally characterized by NMR and ES/MS and considered as a trihydrate according to the elemental analysis.

Different procedures were used for the preparation of the lanthanide(III) complexes. The Eu_2–CS(DO3A-P^{NBn})$_2$ and Y_2–CS(DO3A-P^{NBn})$_2$ complexes were prepared by mixing an aqueous solution of the ligand with a *ca.* 10% molar excess of the appropriate lanthanide(III) chloride. The pH was then adjusted to 7 and the cloudy solution was stirred and heated at 60 °C overnight until it became clear. Then, the Chelex 20 chelating resin in potassium-cycle was added in a batch form to remove the excess free Ln^{3+} ions. In the preparation of the corresponding Gd^{III} complex, the Chelex 20 resin was used in the column form. The presence of free lanthanide(III) ions was checked by the usual xylenol orange test.[26]

The synthesis of the mixed Gd^{III}/Y^{III} complex followed a completely different scheme. The monomeric Gd–DO3A-P^{ABn} complex, prepared according to the published procedure,[14a] was mixed with DO3A-P^{NCS} at pH 9–10 to obtain a mono-Gd^{III} complex of the ditopic ligand. Then, a 50% molar excess of yttrium(III) chloride was added to the solution. To the mixture, stirred at 60–70 °C and pH ~7 overnight, the Chelex 20 was finally added in a batch form. The excess of salts from the solution of the Gd^{III}/Y^{III} ditopic complex was removed by ultrafiltration.

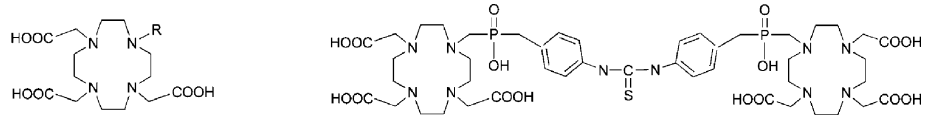

DOTA, R = -CH_2COOH
DO3A-P^{ABn}, R = -CH_2P(O)(OH)Bn-*p*-NH_2
DO3A-P^{NCS}, R = -CH_2P(O)(OH)Bn-*p*-NCS

CS(DO3A-P^{NBn})$_2$

Chart 1 Chemical structures of the ligands.

In order to confirm the complete formation of the ditopic ligand and the formation of the $[Ln_2(CS(DO3A\text{-}P^{NBn})_2)(H_2O)_2]^{2-}$ complexes, we focused on the gadolinium derivative and performed a relaxometric titration of the ligand with $GdCl_3$. To an aqueous solution of the ligand (5 mM) increasing amounts of gadolinium(III) were added and the water proton longitudinal relaxation rate (R_1) measured, at 400 MHz and 298 K. The plot of R_1 *versus* the concentration of Gd^{3+} gives a straight line whose slope corresponds to the relaxivity of the ditopic complex (Fig. S1†).

The relaxivity has a value of 5.7 s^{-1} mM^{-1} (per Gd; 400 MHz, 298 K) which clearly indicates the presence of one coordinated water molecule ($q = 1$) in the inner coordination sphere of each metal ion, as expected. The addition of an excess of $GdCl_3$ causes a steep increase in the value of R_1 because of the different relaxivity of the free Gd^{3+} (11.0 s^{-1} mM^{-1}, under identical experimental conditions). This change is observed at a 2 : 1 Gd/L molar ratio, thus confirming the complete formation of the ditopic complex. The value of the hydration number q was independently assessed by measuring the water ^{17}O NMR chemical shift as a function of the concentration of the Dy_2–$CS(DO3A\text{-}P^{NBn})_2$ complex in the range 5–70 mM (Fig. S2†). The dysprosium(III) induced ^{17}O contact shifts of bound water molecules are, to a very good approximation, independent of structure. Then, these shifts are directly proportional to the value of q.[27] From the slope (−38.5 ppm M^{-1} at 298 K) of the straight line obtained by plotting the ^{17}O shifts as a function of the concentration of Dy^{3+} ion, we can safely attribute a single bound water to each metal ion in the ditopic complex.[28]

NMR solution studies of the $[Eu_2(CS(DO3A\text{-}P^{NBn})_2)(H_2O)_2]^{2-}$ complex

Further insight into the structural properties of the ditopic complexes in aqueous solution was obtained from the ^1H and ^{31}P NMR spectra of the Eu^{III} complex. This metal ion was chosen because its NMR spectra are characterized by a good compromise between a limited paramagnetically induced line broadening and relatively large isotropic paramagnetic shifts. In addition, the information gained is likely to be valid also for the corresponding complexes of gadolinium(III), due to the proximity of the two elements in the Ln series.

It is well known that the Ln^{III} complexes of DOTA-like ligands exist in solution as a mixture of coordination isomers differing in the relative conformation of the macrocyclic ring (λλλλ or δδδδ) and in the orientation of the four pendant arms (Λ or Δ). One isomer has a mono-capped twisted square antiprismatic geometry (TSAP; ***m*** isomer) and the other a mono-capped square antiprismatic geometry (SAP; ***M*** isomer). Generally, the proton NMR spectrum of the ***M*** isomer covers a significantly broader range of chemical shifts than the corresponding ***m*** isomer.[29] Furthermore, the ***m***-type coordination isomer exhibits a much faster rate of water exchange than the ***M***-type complex.[11,30] In our case, the ligand contains a prochiral phosphorus atom in the phosphinic acid pendant arm and then the number of isomeric species in an aqueous solution of the Ln^{III} complexes is expected to increase, because of the presence of *R* and *S* epimers on the phosphorus atom.[31–33] In the case of the parent Eu–DO3A-P^{ABn} complex, the solution ^1H NMR spectrum showed the presence of three isomers: $\boldsymbol{m}_1$, $\boldsymbol{m}_2$ and $\boldsymbol{M}_1$.[14a]

The spectral region of the axial protons of the macrocyclic ring (*ca.* 10–40 ppm) is typically used for the determination of the number of isomeric species.[29] These protons, being very close to the pseudo-C_4 magnetic axis of the complex, are the most shifted. Three sets of four signals are detected in the ^1H NMR spectra of Eu_2–$CS(DO3A\text{-}P^{NBn})_2$ between 273 (Fig. S3†) and 298 K (Fig. 1(a)),

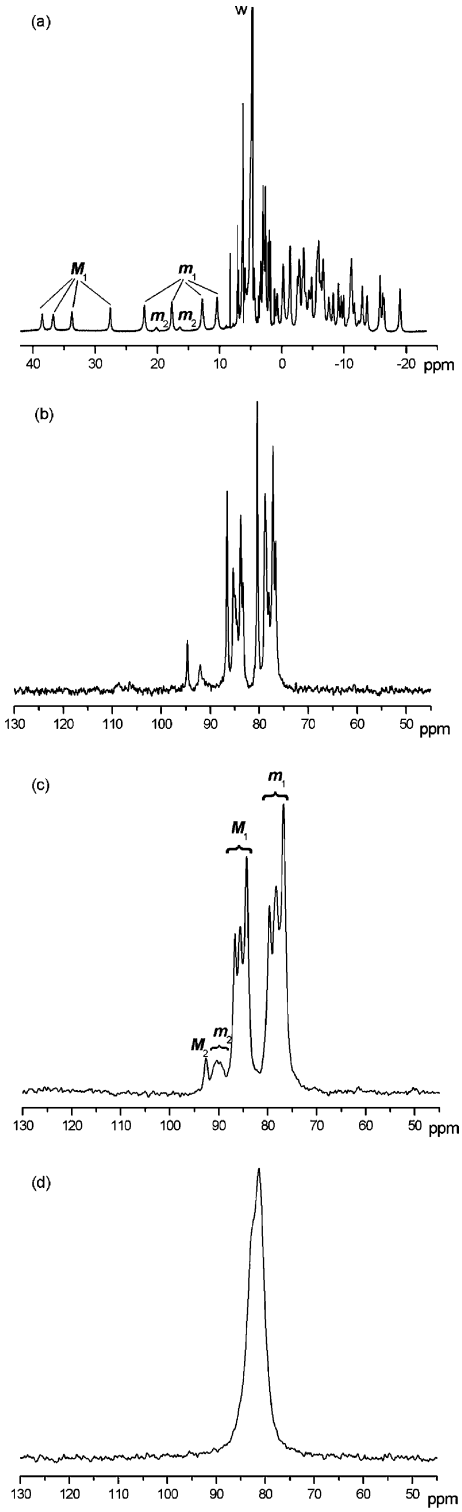

Fig. 1 ^1H NMR spectrum at 298 K (a) and ^{31}P NMR spectra of $[Eu_2(CS(DO3A\text{-}P^{NBn})_2)(H_2O)_2]^{2-}$ at 273 (b), 298 (c) and 363 K (d). All the spectra were recorded at 9.1 T and pH 7.

that correspond to three isomeric species. The four resonances at low field (28.6–38.6 ppm) are easily assigned to an ***M***-type isomer ($\boldsymbol{M}_{R(S)}$), whereas the two set of signals in the range 10.5–22.1 ppm can be attributed to two ***m***-type isomers: $\boldsymbol{m}_{R(S)}$ and $\boldsymbol{m}_{S(R)}$. The relative area of corresponding resonances is correlated to the relative population of the three isomers: $\boldsymbol{m}_{R(S)} : \boldsymbol{M}_{R(S)} : \boldsymbol{m}_{S(R)} \cong 54 : 38 : 8$. The overall ***m*** : ***M*** ratio, estimated from the spectrum recorded at 273 K, was found to be 6 : 4. This value is quite similar to that found for the parent monomeric complex, Eu–DO3A-P^{ABn},[14a] and much higher than for the Eu–DOTA complex.[34]

The ^{31}P NMR spectra were more informative. The spectrum at 298 K (Fig. 1(c)) is rather complex and shows four groups of signals in the range 75–95 ppm. The relative area of the four sets of resonances, calculated after deconvolution of the signals, is *ca.* 55 : 37 : 6 : 2, from high to low field. The strict correspondence of these ratios with those calculated in the proton spectra was the basis of the assignment of Fig. 1(c). By lowering the temperature to 273 K (Fig. 1(b)), the resonances sharpen up and their number increases to 13. On the other hand, the spectrum at 363 K shows only a single, broad peak ($\Delta\nu_{1/2}$ = 500 Hz) centered at 81 ppm (Fig. 1(d)). Clearly, a number of isomeric species exists in solution that mutually interconvert over a broad temperature range. The large number of isomers evidenced by the ^{31}P NMR spectrum at 273 K can be rationalized by assuming that both monomeric units in the ditopic complex behave independently and that each unit may assume four isomeric forms: $\boldsymbol{m}_R$, $\boldsymbol{m}_S$, $\boldsymbol{M}_R$ and $\boldsymbol{M}_S$. It follows that the ditopic complexes may exist in solution as a mixture of ten different isomeric species that could originate up to 16 distinct resonances in the ^{31}P NMR spectra (Table S1, ESI†). This means that, at low temperature, nearly all the possible isomeric species are present in the aqueous solution of [Eu$_2$(CS(DO3A-P^{NBn})$_2$)(H$_2$O)$_2$]$^{2-}$. The isomers may exchange through both arm rotation and inversion of the macrocyclic ring and, as a result, a single exchange-averaged signal is detected in the high temperature limiting spectrum.

The differences between the ^{31}P and the ^{1}H NMR spectra could be explained by three different reasons: (*i*) the phosphorus atom is the origin of the *R*/*S* chirality and is then more sensitive to *R* and *S* isomerism than the axial protons of the macrocyclic ring; (*ii*) since both phosphinate groups are connected by the same thiourea bridge, they are more sensitive to configurational changes occurring at the opposite end of the ditopic complex; (*iii*) the europium(III)-induced ^{31}P NMR isotropic shifts are sensibly larger than the proton ones and this results in a better dispersion of the resonances.

^{1}H and ^{17}O relaxometry

The longitudinal proton relaxivity of the ditopic [Gd$_2$(CS(DO3A-P^{NBn})$_2$)(H$_2$O)$_2$]$^{2-}$ complex is 8.2 s^{-1} mM^{-1}, at 20 MHz and 298 K. This value represents an increase of *ca.* 44% over the relaxivity of the corresponding monomeric complex and it is sensibly higher than those reported for related monoaqua–Gd^{III} dimers. Furthermore, the ^{1}H relaxivity is pH independent in the range 2.5 to 12 (Fig. S4†) in close analogy with the observation made for the monomeric parent [Gd(DO3A-P^{ABn})(H$_2$O)]$^-$ complex.[14a] The constant value of r_1 over a wide pH range indicates that significant structural changes (coordination, hydration or isomerization equilibria) do not occur on passing from alkaline to acidic conditions. Detailed information on the relaxometric properties of the Gd^{III} complex is provided by the measurement of the magnetic-field dependence of the ^{1}H relaxivity (nuclear magnetic relaxation dispersion, NMRD, profiles) and the temperature dependence of the ^{17}O transverse relaxation rate, R_2, of the solvent water. We have measured the ^{1}H NMRD profiles, at 298 and 310 K, from 0.01 to 70 MHz (Fig. 2(b)) and the ^{17}O data at 2.12 T in the range 273–353 K (Fig. 2(a)). The experimental data were analysed by a simultaneous fitting procedure to the well-established Solomon–Bloembergen–Morgan (SBM) equations for the inner-sphere (IS) paramagnetic relaxation and to Freed's model for the outer-sphere (OS) relaxivity. The ^{17}O data were interpreted on the basis of the Swift–Connick equations (for full equations, see ESI†).[1,2,5,35]

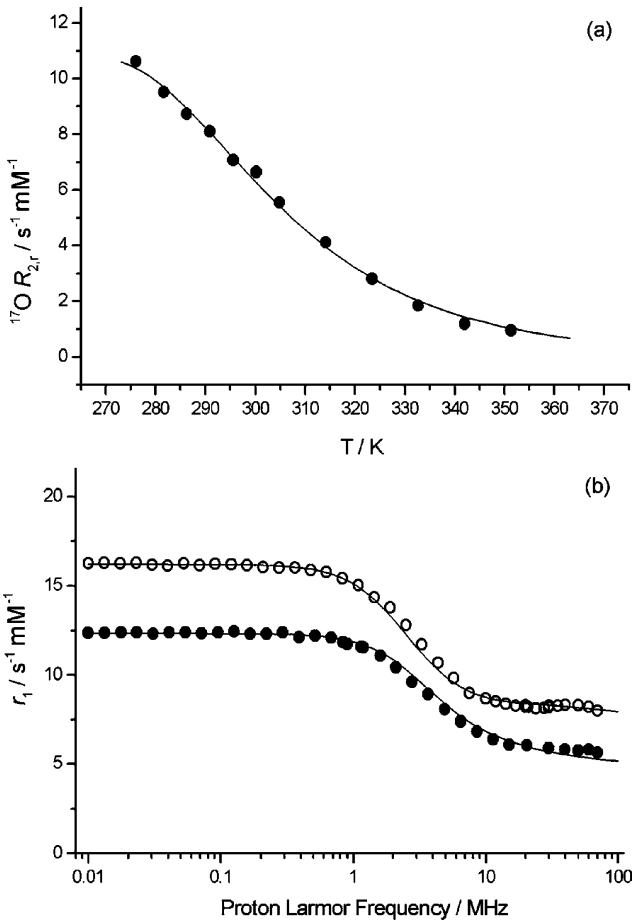

Fig. 2 Relaxometric data of [Gd$_2$(CS(DO3A-P^{NBn})$_2$)(H$_2$O)$_2$]$^{2-}$: (a) ^{17}O transverse relaxation rates normalized to 1 mM concentration, R_{2r} at 2.12 T; (b) ^{1}H NMRD profiles at 298 (open circles) and 310 K (filled circles).

Given the large number (18) of parameters involved, it is customary to fix some of them to reasonable or typical values during the fitting procedure. The hyperfine coupling constant, $A/\hbar$, modulating the Gd–O scalar interaction was fixed to the value found for the related monomeric Gd–DO3A-P^{ABn} complex (-2.9×10^6 rad s^{-1}).[14a] The gadolinium–water oxygen distance (R_{GdO}) and the gadolinium–water proton distance (R_{GdH}) were fixed to 2.6 and 3.1 Å, respectively. These values are slightly longer than those typically used and reflect the presence of the bulky phosphorus acid group that increases the steric interaction with the coordinated water molecule.[14b,13,36] The outer-sphere

Table 1 Results of the multiparametrical simultaneous fitting of ^{1}H NMRD and ^{17}O NMR data. The calculated values are compared with the data published for selected related complexes (structures of the ligands are shown in Charts 1 and 2)

	Gadolinium(III) complex of							
Parameter	CS(DO3A-P^{NBn})$_2$	pip(DO3A)$_2$[c]	bisoxa(DO3A)$_2$[c]	*p*X(DTTA)$_2$[d]	[Fe(tpy-DTTA)$_2$][e]	OHEC[f]	DO3A-P^{ABn}[g]	DOTA[c]
$^{310}r_1$[a]/s^{-1} mM^{-1}	6.1	5.8	4.9	12.8	15.7	3.5	4.2	3.8
$\Delta^2/10^{20}$ s^{-2}	0.23 ± 0.02	0.17	0.21	0.16	0.28	0.92	0.25	0.16
$^{298}\tau_M$/ns	53 ± 5	670	714	111	196	2500	16.2	244
ΔH_M/kJ mol^{-1}	39 ± 4	34.2	38.5	45.4	39.6	30.9	20.6	49.8
$^{298}\tau_R$[b]/ps	183 ± 3	171	106	278	410	208	88	77
E_r/kJ	37 ± 1	20.4	21.7	20.9	23	17.3	29	16.1
$^{298}\tau_v$/ps	15.9 ± 0.2	19	15	34	18.6	11	11.2	11
E_v/kJ	1	1	1	1	1	4.6	1	1
$\delta g^2_L/10^{-2}$	8 ± 0.3	4	2.8	8	9.5	—	—	—
$A\hbar^{-1}/10^6$ rad s^{-1}	−2.89	−3.8	−4.2	−3.6	−3.7	−3.7	−2.89	−3.7
R_{GdO}/Å	2.6	2.5	2.5	2.5	2.5	2.5	2.6	2.38
R_{GdH}/Å	3.1	3.1	3.1	3.1	3.1	3.1	3.1	—
R_{GdGd}/Å	6.3	~8	~8	—	12.5	6.5	—	—
A/Å	3.6	3.5	3.5	3.5	3.5	4.5	3.6	—
ΔH_{Mss}/kJ	10	—	—	—	—	—	15	—
$^{298}\tau_{Rss}$/ps	23 ± 3	—	—	—	—	—	9	—
R_{ss}/Å	3.5	—	—	—	—	—	3.6	—
$^{298}\tau_{Mss}$/ns	1	—	—	—	—	—	1	—
q	1	1	1	2	2	1	1	1
q_{ss}	1	—	—	—	—	—	1	—

[a] Values at 20 MHz. [b] The τ_R values reported here represent rotational correlation times of the Gd–H vector (τ_R(H)). Where only τ_R(O) values were published, the corresponding values of τ_R were calculated from τ_R(O) and the τ_R(H)/τ_R(O) ratio. [c] Ref. 18. [d] Ref. 24*d*. [e] Ref. 24*c*. [f] Ref. 39. [g] Ref. 14*a*.

contribution is controlled by the distance of shortest approach, A, of the bulk water molecules to the gadolinium(III) ion and the relative diffusion coefficient, of the water molecules and the complex, D_{GdH}. The distance A was fixed to 3.6 Å, whereas the value of D_{GdH} was calculated according to the semi-empirical Hindman's equation.[37] However, the analysis of the data only in terms of the standard inner- and outer-sphere contributions was far from being satisfactory. In particular, the experimental NMRD profiles could not be reasonably reproduced. As for the corresponding monomeric derivative, also a contribution to the proton relaxivity from the water molecules hydrogen-bonded to the polar groups of the ligand had to be taken into account (the second-sphere contribution). This is often observed in the case of phosphorus-containing groups that are highly hydrophilic and able to participate in tight hydrogen-bonding interactions with a number of water molecules near the paramagnetic center.[16] This contribution depends on the number of water molecules in the second coordination sphere, q_{ss}, their average distance from the metal center, R_{ss}, their mean residence lifetime, τ_{Mss}, and the rotational correlation time of the vector joining the Gd^{3+} ion to the protons of these water molecules, τ_{Rss}. The hydration number q_{ss} was set to 1, in accordance with the choice made for the monomeric complex,[14a] the residence lifetime $^{298}\tau_{Mss}$ was fixed to the very short value of 1 ns,[38] and R_{ss} to 3.5 Å. By considering the second-sphere contribution (SS) to the relaxivity the experimental data could be nicely reproduced (Fig. 2) following a well established procedure (for full equations, see ESI†).[14a]

The best-fit parameters are summarized in Table 1 and compared with those published for Gd–DOTA, Gd–DO3A-P^{ABn} and a few selected multimeric complexes. Perhaps the most striking characteristics of Gd$_2$–CS(DO3A-P^{NBn})$_2$ is the short value of the residence lifetime of the coordinated water molecule as compared to the other complexes listed in Table 1. The value of $^{298}\tau_M$ is more than one order of magnitude shorter with respect to the ditopic complexes with $q = 1$ and shorter by a factor of 2–4 with respect to the multimeric complexes with $q = 2$. On the other hand, the exchange lifetime of [Gd$_2$(CS(DO3A-P^{NBn})$_2$)(H$_2$O)$_2$]$^{2-}$ is more than three times longer than that for the related monomeric complex:[14a] 53 and 16 ns, respectively, at 25 °C. This could be an effect associated with a different structure and/or dynamics of the second hydration sphere for the monomeric and ditopic complexes. In fact, an hydrophilic amino group in DO3A-P^{ABn} is replaced by a hydrophobic thiourea bridge in CS(DO3A-P^{NBn})$_2$. On the other hand, the different water accessibility of the two complexes as a result of their different solution structures (*vide infra*) cannot be excluded. In any case, the water exchange rate of the gadolinium dimer is rather close to the optimal range of values (*ca.* 20–40 ns) predicted by the theory and thus fast enough so as not to limit the relaxivity. At the physiological temperature and at the frequencies of clinical use (20–60 MHz), the relaxivity of the Gd^{III} complexes of medium-low molecular weight is mostly controlled by their rotational dynamics. An inspection at the rotational correlation times ($^{298}\tau_R$) of the ditopic complexes of Table 1 shows that the value found for [Gd$_2$(CS(DO3A-P^{NBn})$_2$)(H$_2$O)$_2$]$^{2-}$ (183 ps) is significantly longer than that of Gd$_2$–bisoxa(DO3A)$_2$ (106 ps),[18] a complex featuring a rather flexible oxoethylene linker, and very similar to that of [Gd$_2$(pip(DO3A)$_2$)(H$_2$O)$_2$] (171 ps),[18] a complex characterized by the presence of a rigid cyclic bridging moiety. Moreover, $^{298}\tau_R$ of 183 ns is just about two times longer than that found for the parent Gd–DO3A-P^{ABn} complex (88 ps).[14a] So, the twofold increase in molecular weight on passing from the monomer to the dimer is closely mirrored by a twofold decrease in the molecular tumbling rate, thus suggesting for the ditopic complex a compact solution structure and a restricted internal motion about the thiourea spacer. This can be seen in Fig. 3 where the different contributions to the relaxivity are plotted

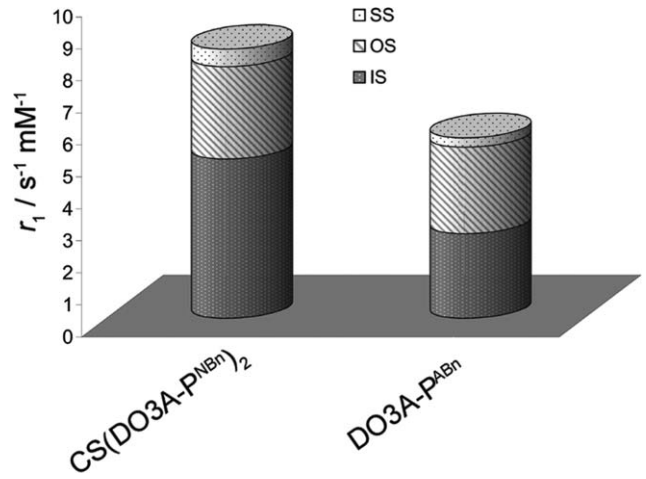

Fig. 3 Comparison of proton relaxivities of Gd_2–(CS(DO3A-P^{NBn})$_2$ and Gd–DO3A-P^{ABn} complexes (25 °C, 20 MHz). The overall values are depicted in the form of stacked bars representing the sum of the inner- (IS), second- (SS) and outer-sphere (OS) contributions.

for the monomeric and ditopic complexes. The IS term for the dimer is two times larger than for the monomer, whereas the OS contribution is about the same for the two complexes.

To the best of our knowledge, the ^{1}H relaxivity of $[Gd_2(CS(DO3A\text{-}P^{NBn})_2)(H_2O)_2]^{2-}$ (8.2 s^{-1} mM^{-1}, at 298 K and 20 MHz) is the highest so far reported for low-molecular weight dinuclear complexes with $q = 1$. The reasons for this are the optimization of the water exchange rate, the lack of fast local motions and the presence of a sizeable contribution of the second hydration sphere. The SS term makes a contribution of *ca.* 7% to the relaxivity of both the mono- and dinuclear gadolinium complexes (Fig. 3).

Finally, we checked the possible influence of intramolecular Gd^{3+}–Gd^{3+} interactions in the ditopic complex on the relaxivity. Merbach *at al.* have recently reported an enhancement of the electron spin relaxation arising from this effect for the dinuclear gadolinium(III) complex of the macrocyclic ligand OHEC (H_8OHEC = octaazacyclohexacosane-1,4,7,10,14,17,20,23-octaacetate; Chart 2) where the distance between the paramagnetic ions is about 6.5 Å.[39] A more rapid electronic relaxation might affect the relaxivity and limit its enhancement obtained by increasing the rotational correlation time. In the absence of EPR data,[24c,40] we checked the possible influence of magnetic coupling between the Gd^{3+} ions by comparing the ^{1}H NMRD profiles of the homo- and heterodinuclear $[Gd_2(CS(DO3A\text{-}P^{NBn})_2)(H_2O)_2]^{2-}$ and [GdY(CS(DO3A-P^{NBn})$_2$)$(H_2O)_2]^{2-}$ complexes, at 298 K and 310 K (Fig. 4). The

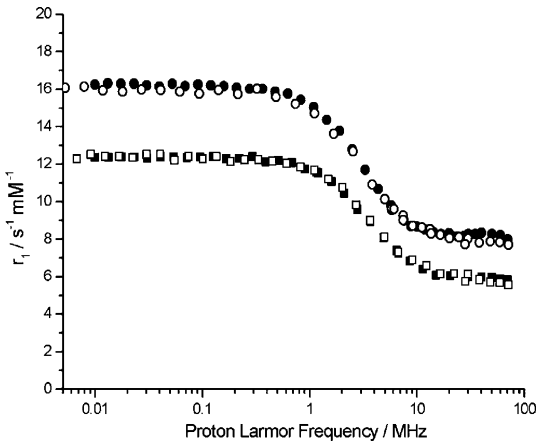

Fig. 4 ^{1}H NMRD profiles of Gd_2–(CS(DO3A-P^{NBn})$_2$ (filled symbols) and GdY–(CS(DO3A-P^{NBn})$_2$ (open symbols) complexes at 298 (circles) and 310 K (squares).

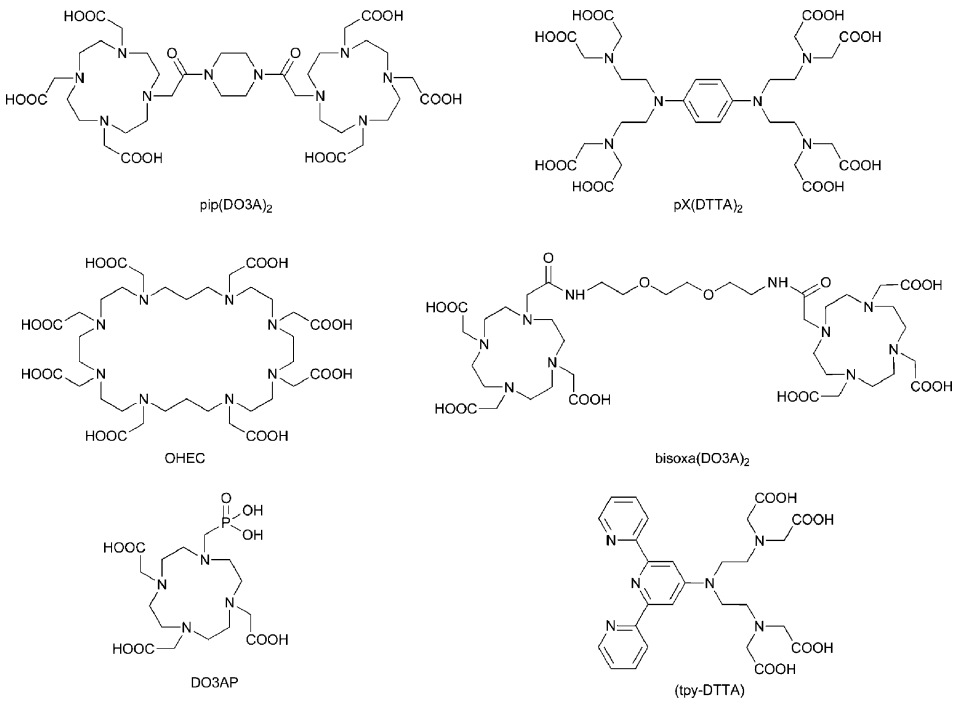

Chart 2 Chemical structures of the ligands discussed in the text and in Table 1.

relaxivity of the two complexes is nearly identical at both temperatures and over the entire range of magnetic fields investigated. It follows that the intramolecular interactions involving the Gd^{3+} ions can be neglected since they do not have any influence on the relaxivity of the ditopic complex.

NMR solution study of the homonuclear Y^{III}/Y^{III} and heteronuclear Gd^{III}/Y^{III} complexes

The long τ_R value suggests for the dimer a rather isotropic tumbling motion without a large contribution from local rotation about the bridge connecting the two paramagnetic units. This opens up the problem of assessing the solution structure of the complex.

From molecular modeling, the possible range of Ln···Ln distances in solution can be easily determined: from 21 Å for a totally stretched conformation to 5.5 Å for the most compact structure. In order to get some information on the actual structure of the ditopic complex in aqueous solution, we prepared the mixed Gd^{III}/Y^{III} species and used the ^{89}Y isotope as a reporting NMR nucleus and the gadolinium(III) ion as a paramagnetic probe.

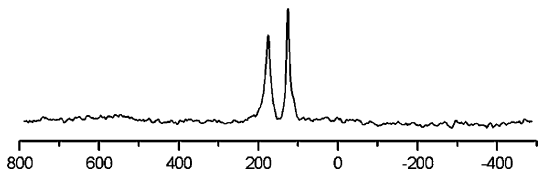

Fig. 5 ^{89}Y NMR spectrum of $[GdY(CS(DO3A\text{-}P^{NBn})_2)(H_2O)_2]^{2-}$ at 9.1 T and 298 K.

The ^{89}Y NMR spectrum of the heteronuclear Gd^{III}/Y^{III} complex, at 9.1 T and 298 K, consists of two peaks separated by *ca.* 49 ppm in the relative ratio of 4 : 5 (Fig. 5). Since an unambiguous assignment of the resonances is not possible, the signals were tentatively attributed on the basis of the comparison with the proton NMR spectrum of the Eu^{III} complex and on the expectation that the population of the ***m***-type isomeric species increases across the lanthanide series.[34] So, the signals at 126.3 and 175.4 ppm were assigned to the ***M*** and ***m*** isomers, respectively. Likely, the broadening at the bottom of these resonances may be indicative of contributions arising from the occurrence of various isomeric species as discussed above. Then, we measured the Gd^{3+}-induced decrease of the T_1 relaxation times of the two ^{89}Y signals in order to estimate the Gd···Y distance. The ^{89}Y longitudinal relaxation times are primarily dominated by the dipolar interaction, as the through-bond (contact) contribution is negligible because of the large distance separating the two metal ions. With the further assumption that the motion in solution is isotropic, the following simplified Solomon–Blombergen equation can be used:[41]

$$\frac{1}{T_{1,p}} = \frac{2}{5}\left(\frac{\mu_0}{4\pi}\right)^2 \frac{\gamma_I^2 \mu_{eff}^2 \beta^2}{r^6} \tau_R \qquad (1)$$

In eqn (1), $\mu_0/4\pi$ represents the magnetic permeability of a vacuum (1×10^{-7} H m^{-1}), γ_I is the gyromagnetic ratio for ^{89}Y (1.32×10^7), μ_{eff} is the effective magnetic moment of Gd^{3+} ($7.94\,\mu_B$), β is the Bohr magneton, r is the metal–metal distance and τ_R the rotational correlation time of the complex (183 ps, from NMRD and ^{17}O data). For the two ^{89}Y NMR peaks we measured relaxation times of 0.088 and 0.076 s that correspond to Gd···Y distances of 6.3 and 6.2 Å, respectively. This result confirms the hypothesis that the dimer adopts, in aqueous solution, a rather compact structure with the two terminal DOTA-like subunits close to each other.

Additional information is provided by the ^{13}C T_1 relaxation times of the heteronuclear Gd^{III}/Y^{III} complex. The ^{13}C NMR spectrum (Fig. 6) can be partially assigned by comparison with the spectrum of the pure ligand (Fig. S5†) owing to the lack of pseudocontact contribution of the Gd^{3+} ion to the lanthanide-induced shift (LIS).[41] Three groups of signals can be distinguished: (*i*) CH_2 carbons of the macrocycle ring and of the pendant arms, (*ii*) aromatic carbons and (*iii*) carbonyl and thiocarbonyl carbons. As the carbon atoms of the gadolinium-containing macrocyclic subunit are at a distance shorter than 3.5 Å from the paramagnetic centre, their resonances are not visible in the NMR spectrum because of the exceedingly large line broadening. Thus, the spectrum of Fig. 6 contains only signals corresponding to carbon atoms of the yttrium-containing subunit. The ^{13}C T_1 relaxation times were measured with the standard inversion recovery technique using a $\pi/2$ pulse of 12 μs and their mean value was about 0.015 s. From this an average distance of 8.2 Å from the Gd^{3+} ion can be calculated from eqn (1) (for a complete list of relaxation times see Tables S1 and S2†).

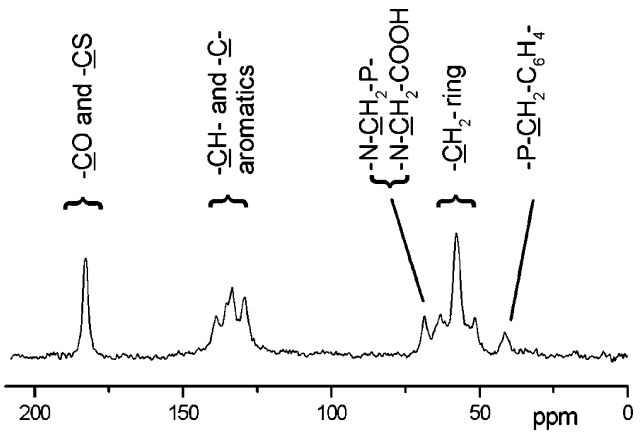

Fig. 6 ^{13}C NMR spectra of $[GdY(CS(DO3A\text{-}P^{NBn})_2)(H_2O)_2]^{2-}$ at 9.1 T, 298 K and pH 7. The assignment is based on the comparison with the ^{13}C NMR spectrum of the free $CS(DO3A\text{-}P^{NBn})_2$ ligand.

Besides the approximations involved in the procedure used, it is worth noting that the calculated interatomic distances only represent mean values over all the isomeric species that are present in aqueous solution. In any case, the distance data obtained point to a structure where the two metal centres are spatially close, in agreement with the results of the analysis of the relaxometric data. An approximate solution structure of the ditopic complex can be obtained by molecular modeling simulations using as constraints the Gd···Y distance of 6.25 Å and the average Gd···C distance of 8.2 Å. The only result that could satisfy both conditions involves a face-to-face arrangement of the two O4-planes of the coordination polyhedrons (Fig. 7). In such a geometry the dimer shows a rather spherical shape which accounts for the prevalent isotropic reorientational dynamics in solution and a limited presence of independent rotational motions of the two terminal subunits. This conformational geometry might be stabilized by the presence of hydrogen bonding interactions

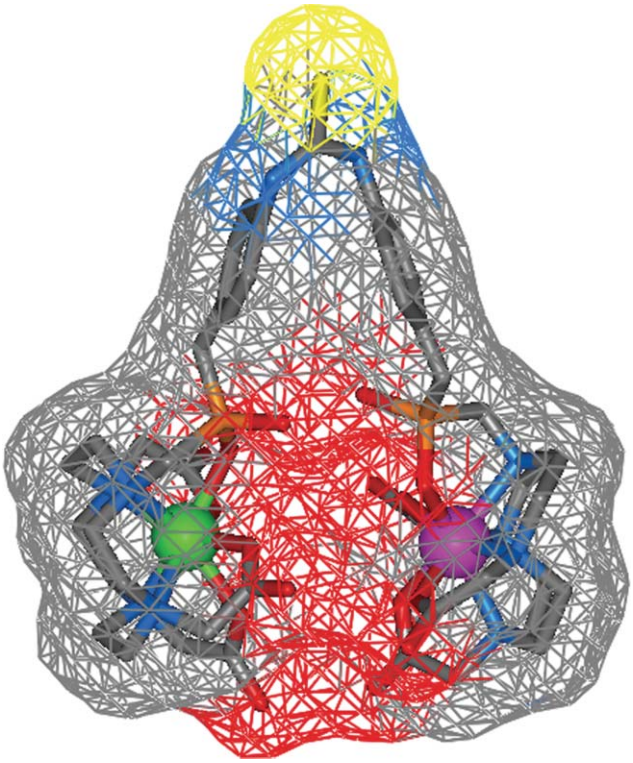

Fig. 7 Proposed solution structure of the $[GdY(CS(DO3A\text{-}P^{NBn})_2)(H_2O)_2]^{2-}$ complex in solution obtained from molecular modeling. The colours of the atoms are the following: Y (green), Gd (magenta), O (red), N (blue), P (orange), S (yellow) and C (gray). The network represents the solvent accessibility surface of the molecule. The coordinated water molecules were included into the simulation but they are omitted in the picture for clarity. The ionic radii of the Ln^{3+} ions are not to scale and are just a guide to the eyes.

involving the phosphinate oxygen atoms. In fact, a rich network of hydrogen bonds has been observed in the solid state structure of the lutetium(III) complex of the monophosphonic acid analogue of DOTA (H_5DO3A-P, Chart 2),[36] where pairs of complexes are orientated face-to-face in an arrangement quite similar to that proposed for the ditopic species. In addition, the solvent accessibility surfaces calculated using the water molecule as a probe (1.4 Å in diameter) indicate that both coordination centers are easily accessible to the water molecules. This result is also in good agreement with the fast rate of water exchange of the coordinated water molecule.

Conclusion

We have synthesized a new "ditopic" phosphorus-containing ligand, $CS(DO3A\text{-}P^{NBn})_2$, characterized by two terminal macrocyclic subunits joined with a thiourea linker commonly used for the preparation of high-molecular-weight or targeted MRI CA. In the corresponding lanthanide(III) complexes, the two metal ions are nine-coordinate with one inner-sphere water molecule. In aqueous solution the complexes are present as a mixture of stereoisomers mutually interconverting at high temperature. At room temperature, the ^{1}H NMR spectrum of the Eu^{III} derivative indicates the prevalence of isomeric species with a twisted square antiprismatic geometry (***m***-type isomer). This isomeric form is known to be endowed with a rate of exchange of the coordinated water molecule, k_{ex}, faster than that of the related ***M***-type isomer. In fact, the rate of exchange found is the highest measured for dinuclear Gd^{III} complexes: $^{298}k_{ex} = (1.9 \pm 0.2) \times 10^7\ s^{-1}$. The high relaxivity of the $[Gd_2(CS(DO3A\text{-}P^{NBn})_2)(H_2O)_2]^{2-}$ complex is explained by the presence of a sizeable contribution from water molecules hydrogen-bonded to the phosphinate groups and by a reorientational motion of the complex largely isotropic. This latter property is highly relevant as most of the ditopic complexes reported are characterized by a relaxivity limited by the presence of a relatively fast local rotation about the linker joining the two terminal subunits. The relatively rigid and compact structure of the ditopic complexes is explained on the basis of a favoured conformation in solution where the two terminal macrocyclic chelates are facing each other with the metal ions at a distance of *ca.* 6.3 Å. This conformation is stabilized by a network of hydrogen-bonding interactions involving the phosphinate groups and the water molecules.

The high water solubility, stability, rate of water exchange and relaxivity make the new dinuclear $[Gd_2(CS(DO3A\text{-}P^{NBn})_2)(H_2O)_2]^{2-}$ complex a promising candidate for the preparation of multimeric (*e.g.* dendrimeric) conjugates for molecular imaging applications.

Experimental

Ligand synthesis

Reagents and solvents were purchased from commercial sources with the highest quality grade and were used as received. The starting ligand $DO3A\text{-}P^{ABn}\cdot 3H_2O$ was synthesized according to the literature procedure.[14a] TLC was performed on Kieselgel 60 F_{245} aluminium sheets with fluorescence indicator (Merck) in *i*PrOH/acetic acid/water 6 : 1 : 8 mixture with detection using UV irradiation, ninhydrin spray or iodine vapour. Elemental analyses were performed at the Institute of Macromolecular Chemistry of the Czech Academy of Science (Prague). The ^{1}H, ^{13}C and ^{31}P NMR spectra were recorded on a Varian ^{UNITY}*INOVA* 400 spectrometer. ES/MS spectra were run on Bruker ESQUIRE 3000 equipment with ion-trap detection in positive or negative modes.

1,4,7,10-Tetraazacyclododecane-4,7,10-triacetice-1-{methyl[(4-isothiocyanatophenyl)methyl]phosphinic acid} (DO3A-P^{NCS}). The aminobenzylic derivative $DO3A\text{-}P^{ABn}$ hydrate (0.5 g, 0.856 mmol) was dissolved in 5 ml of water in a 20 ml plastic (PE) vessel. The pH value was then adjusted to 2–3 (detected by universal pH-test paper) by addition of concentrated hydrochloric acid. In the next step, thiophosgene (88 µl, 1.03 mmol, purity ~90%) in tetrachloromethane (5 ml) solution was added and the vessel was quickly capped and sealed with parafilm. The mixture was vigorously shaken in a horizontal position overnight. The course of the reaction was followed by TLC with ninhydrin detection until the violet-red spot of the starting amine ($R_f = 0.3$) had disappeared. The water phase was extracted with CCl_4 (2 × 5 ml) and Et_2O (2 × 5 ml) and evaporated to dryness yielding crude isothiocyanate $DO3A\text{-}P^{NCS}$ in the form of a solidified glass. This glass was ground to a powder and the excess hydrochloric acid in the powder was removed by vacuum-pumping (2.7 kPa, 5 h, 50 °C) to afford the target product (0.55 g, yield 90%). This form of the isothiocyanate was used in further reactions or it was

purified by flash chromatography on a short silica gel column with *i*PrOH/acetic acid/water 6 : 1 : 8 elution for characterization purposes. TLC (UV, iodine vapour): $R_f = 0.45$. Found: C, 38.01; H, 5.93; N, 10.10; S, 4.54. $C_{23}H_{34}N_5O_8PS{\cdot}4HCl$ (M = 717.4) requires C, 38.51; H, 5.34; N, 9.76; S, 4.47%. NMR δ_H (400 MHz, D_2O, 25 °C; *t*BuOH): 2.87–3.90 (24H, m, ring and pendant $-CH_2-$); 7.20 (2H, m, aryl); 7.23 (2H, m, aryl); δ_C (100.6 MHz, D_2O, 25 °C; *t*BuOH): 53.6 (1C, d, $^1J_{CP}$ 79.8, P–CH_2–C_6H_4); 54.9, 55.8, 56.7 (6C, $-CH_2-$ ring); 57.5 (1C, d, $^1J_{CP}$ 82, N–CH_2–P); 58.3 (2C, –CH_2–COOH); 58.9 (2C, $-CH_2-$); 59.7 (–CH_2–COOH); 131.1 (2C, d, J_{CP} 2.6, aryl CH); 134.5 (1C, d, J_{CP} 3.8, aryl C); 136.2 (2C, d, J_{CP} 5.3, aryl CH); 136.8 (1C, bs, –N=*C*=S); 139.3 (1C, aryl C); 173.6 (1C, –*C*OOH); 179.7 (2C, –*C*OOH); δ_P (161.9 MHz, D_2O, 90 °C; ext. 85% H_3PO_4): 29.8 (bs). ESI/MS: m/z 572.4 $(M + H)^+$, $C_{23}H_{34}N_5O_8PS$ requires 572.6; 361.3 $(M - CH_2 - P^{NCS})^+$, $C_{15}H_{27}N_4O_6$ requires 360.4.

CS(DO3A-P^{NBn})$_2$. A portion of the DO3A-P^{ABn} hydrate (0.5 g, 0.856 mmol) was dissolved in 5 ml of water. Subsequently, the DO3A-P^{NCS} hydrochloride (0.675 g, 0.942 mmol, 1.1 eq.) was added and the pH was adjusted to 9–10 by addition of aqueous 1.5 M KOH. This reaction mixture was then stirred overnight at RT. The crude product was purified by chromatography on cationic exchange resin Amberlite CG50 (100–200 mesh) in H^+-form with water elution. In the first fractions, only hydrochloric acid was eluted, whereas the pure product was eluted in the later fractions. At the end, traces of unreacted DO3A-P^{ABn} were washed out. Product-containing fractions were unified, dissolved in a minimal amount of water (5 ml) and the solution added dropwise to a large excess of anhydrous EtOH (500 ml). The white precipitate was left to mature overnight, filtered off and dried under vacuum. The pure product was obtained as a white solid (0.844 g, 83%). TLC (UV, iodine vapour): $R_f = 0$. Found: C, 45.53; H, 6.54; N, 10.73; S, 4.00. $C_{23}H_{35}N_5O_8PS{\cdot}3H_2O$ (M = 1154) requires C, 45.98; H, 6.35; N, 10.38; S, 3.96%. NMR δ_H (400 MHz, D_2O, 25 °C; *t*BuOH): 3.03 (4H, d, P–CH_2–C_6H_4, J_{HP} 16.4); 3.16–3.50 (36H, m, ring CH_2 + N–CH_2–P); 3.56 (4H, N–CH_2COOH); 3.71 (8H, N–CH_2COOH); 7.31 (4H, m, aryl); 7.36 (4H, m, aryl); δ_C (100.6 MHz, D_2O, 45 °C; EtOH): 41.6 (2C, d, J_{CP} 86.2; –P–CH_2–C_6H_4); 53.1, 52.6 (16C, ring $-CH_2-$); 53.9 (2C, d, J_{CP} 85.5, N–CH_2–P); 57.7 (2C, N–CH_2–COOH); 58.1 (4C, N–CH_2–COOH); 129.2 (4C, aryl CH); 133.2 (4C, d, J_{CP} 4.6, aryl CH); 136.1 (2C, d, J_{CP} 7.2, aryl C); 138.4 (2C, aryl C); 173.6 (4C, –*C*OOH); 178.3 (2C, –*C*OOH); 182.3 (1C, NH–*C*(S)–N); δ_P (161.9 MHz, D_2O, 90 °C; ext. 85% H_3PO_4): 32.7 (bs). ESI/MS: m/z 1099.8 $(M + H)^+$, $C_{23}H_{35}N_5O_8PS$ requires 1102.1; 361.3 $(DO3A - CH_2)^+$, $C_{15}H_{27}N_4O_6$ requires 360.4.

Synthesis of lanthanide(III) complexes and NMR sample preparation

Lanthanide(III) chloride hydrates were purchased from Aldrich, Strem or Alfa. If not stated otherwise, all NMR measurements were carried out in deuterium oxide (99.95% or 99.98% D) received from Chemtrade (Germany).

[Ln$_2$(CS(DO3A-P^{NBn})$_2$)(H$_2$O)$_2$]$^{2-}$ complexes in the solid state (Ln = Y, Eu, Gd). The ligand CS(DO3A-P^{NBn})$_2$ hydrate (0.1 g, 0.086 mmol) was dissolved in water (2 ml). Then, appropriate lanthanide(III) chloride hydrate (1.1 eq.; 0.95 mmol) was added and the pH of the solution was slowly adjusted to 7 with dilute KOH solution and re-adjusted to this value until the pH value was stable. The resulting cloudy mixture was stirred at 60 °C for 12 h. To remove the excess lanthanide(III) ions, the mixture was concentrated using a vacuum evaporator and chromatographed on a short column (Gd) or just stirred with a small batch (Y, Eu) of chelating resin Chelex 20 (Fluka) in K^+-form. The pure complex was eluted with water in one fraction. The fraction was evaporated under vacuum to dryness leaving a glassy/powder solid. For high-resolution NMR measurements (Y_2- and Eu_2-complexes), 20 mM solutions were prepared by dissolving about 30 mg of the solid complex in D_2O (1 ml) followed by filtration through a 20 μm syringe filter into an NMR tube.[26]

[Gd(DO3A-P^{ABn})(H$_2$O)]$^-$ complex solution. The DO3A-P^{ABn} hydrate (0.49 g, 0.839 mmol) was dissolved in water (5 ml) and $GdCl_3{\cdot}6H_2O$ (0.468 g, 1.26 mmol, 1.5 eq.) was added. The pH value was then adjusted to 7 with KOH solution and the mixture was stirred and heated at 60 °C overnight. The excess of Gd^{3+} was removed on a cation exchange column (Amberlite CG50 in H^+-cycle) with water elution: the lanthanide(III) salts were eluted first in acidic fractions whereas the pure complex was found in the following neutral fractions. ESI/MS: m/z (Gd isotopic pattern) 681.1, 681.8, 682.5, 683.2, 685.1 $(M)^-$, $C_{22}H_{36}N_5O_8PGd$ requires 685.8 (for an average Gd atomic mass).

[Gd(CS(DO3A-P^{NBn})$_2$)(H$_2$O)$_2$]$^{2-}$ complex solution. The [Gd(DO3A-P^{ABn})(H$_2$O)]$^-$ complex[14a] (0.5 g, 0.728 mmol) was dissolved in water (5 ml) and the DO3A-P^{NCS} hydrochloride (0.548 g, 0.764 mmol, 1.05 eq.) was added. The solution pH value was immediately adjusted to 9–10 with diluted KOH solution and the solution was stirred overnight at RT. The reaction was monitored by TLC and isothiocyanate was added in small portions over an interval of 6 h until the Gd–DO3A-P^{ABn} TLC spot had disappeared. This solution of the complex was used directly for further reactions. ESI/MS: m/z (Gd isotopic pattern) 1253 $(M)^-$, $C_{45}H_{70}N_{10}O_{16}P_2SGd$ requires 1257; 1292 $(M + K)^-$, $C_{45}H_{70}N_{10}O_{16}P_2SGdK$ requires 1296 (for average Gd atom mass).[42]

[GdY(CS(DO3A-P^{NBn})$_2$)(H$_2$O)$_2$]$^{2-}$ complex. To the reaction mixture containing the [Gd(CS(DO3A-P^{NBn})$_2$)(H$_2$O)]$^{2-}$ complex obtained in the previous reaction, solid YCl_3 hydrate (0.43 g, 1.5 eq. based on the amount of DO3A-P^{NCS}) was added stepwise. In each step, the pH value was re-adjusted to 7 by addition of aq. KOH. The resulting mixture was subsequently heated (60 °C) and stirred for 12 h. Then, the solution was left to cool down and a batch of Chelex 20 resin was added (100 mg per 5 ml). After stirring the mixture overnight at RT, all of the solids were filtered off and the clear solution was ultrafiltered on an Amicon cell through a YC-05 membrane (M_w-cut-off ~500) at 4 atm to remove any inorganic salts. The overall filtrate volume was about 500 ml. The supernatant containing the mixed Gd^{III}/Y^{III} complex and traces of the bis-Y^{III} complex was evaporated under vacuum to yield a glassy powdered solid. ESI/MS: m/z 669.6 $(M)^{2-}$, $C_{45}H_{70}N_{10}O_{16}P_2SGdY$ requires 670.

^{89}Y NMR measurements

For the ^{89}Y measurements, a VT-low-frequency 10 mm probe of the Varian 400 MHz system was utilized. The spectrometer was tuned and the spectra referenced to a 1 M aqueous solution of $Y(NO_3)_3$

(δ_Y = 0 ppm) containing 1 mol% $GdCl_3$. For the measurement of the mixed Y^{III}/Gd^{III} complex, a 0.5 M aqueous solution in a 10 mm tube (overall volume about 2 ml) was utilized. The ^{89}Y T_1 relaxation times were measured by the standard inversion recovery technique with 0.5 s repetition time (d1) and pulse delay (d2) incremented in the range 0.0003–0.154 s to 9 exponentially sampled points. For each increment about 6000 transients were accumulated. Measurements were done at 25 °C and pH 7.

^{1}H relaxation measurements and ^{1}H NMRD profiles

The water proton NMRD profiles were measured at 25 and 37 °C with a Stelar Spinmaster Spectrometer FFC-2000 (Mede, Pv, Italy) on about 1 mmol gadolinium solutions in non-deuterated water. The exact concentration of the solutions was determined by measurement of the bulk magnetic susceptibility shifts of a ^{t}BuOH signal.[43] The ^{1}H T_1 relaxation times were acquired by the standard inversion recovery method with typical 90° pulse width of 3.5 μs, 16 experiments of 4 scans. The reproducibility of the T_1 data was ±5%. The temperature was controlled with a Stelar VTC-91 airflow heater equipped with a calibrated copper-constantan thermocouple (uncertainty of ±0.1 °C). The NMRD profiles were measured over a range of magnetic fields from 0.00024 to 1.6 T (corresponding to 0.01–70 MHz proton Larmor frequencies).

^{17}O relaxation measurements

Variable-temperature ^{17}O NMR relaxation measurement were performed on a JEOL EX-90 (2.1 T, 12.2 MHz) spectrometer with external locking system (D_2O). Experimental settings were: spectral width 10 000 Hz, pulse width 7 μs (90°), acquisition time 10 ms, 2048 scans and no sample spinning. The complex solutions were enriched by addition of $H_2{}^{17}O$ (6%, Yeda, Israel) to give *ca.* 0.2% ^{17}O concentration. Transversal ^{17}O NMR relaxation rates, R_2, were calculated from the line-width at half-height of the ^{17}O signals. The ^{17}O R_2 data were measured from 0–90 °C with 10 °C increments. In order to stabilize the temperature, the samples were maintained in the probe for at least 10 min prior to the measurements being taken.

Best fitting procedure

The analysis of the ^{1}H NMRD and ^{17}O NMR T_2 data were performed with Micromath Scientist[44] fitting routines based on SBM, Freed and Swift–Connick equations (refer to ESI†).[1,2,5,35] All the data were pre-processed and post-processed in Microcal Origin.[45]

Molecular modeling and graphical export

Molecular modeling was carried out using the Hypercube Hyperchem 6.01 program package with the MM+ force-field taking into account only bond dipoles.[46] The final data were then exported to MSI WebLab ViewerPro 4.0 where the solvent accessibility surfaces were also calculated.[47]

Acknowledgements

The authors are thankful to Vojtěch Kubíček and Dr David Sýkora for the measurement of the mass spectra. We are grateful to the GAČR (grant No. 203/03/0168), GAUK (423/2004/B-CH/PrF) and MIUR (FIRB). M. B., P. H. and J. R. gratefully acknowledge the invaluable support of a NATO travel grant (No. PST.CLG 980045). The work was carried out within the frame of COST D18 and the EU-supported NoE projects EMIL (No. LSHC-2004-503569) and DiMI (No. LSHB-2005-512146).

References and notes

1 *The Chemistry of Contrast Agents in Medical Magnetic Resonance Imaging*, ed. A. E. Merbach and É. Tóth, Wiley, Chichester, UK, 2001.
2 *Topics in Current Chemistry*, Springer Verlag, Heidelberg, 2002, vol. 221.
3 P. Caravan, J. J. Ellison, T. J. McMurry and R. B. Laufer, *Chem. Rev.*, 1999, **99**, 2293.
4 S. Aime, M. Botta and E. Terreno, *Adv. Inorg. Chem.*, 2005, **57**, 173.
5 S. Aime, M. Botta, M. Fasano and E. Terreno, *Acc. Chem. Res.*, 1999, **32**, 941.
6 S. Aime, C. Cabella, S. Colombatto, S. G. Crich, E. Gianolio and F. Maggioni, *J. Magn. Reson. Imag.*, 2002, **16**, 394.
7 M. Woods, Z. Kovacs and A. D. Sherry, *J. Supramol. Chem.*, 2002, **2**, 1.
8 V. J. Venditto, C. A. S. Regino and M. W. Brechbiel, *Mol. Pharm.*, 2005, **2**, 302.
9 (*a*) S. Laus, R. Ruloff, É. Tóth and A. E. Merbach, *Chem. Eur. J.*, 2003, **9**, 3555; (*b*) R. Ruloff, É. Tóth, R. Scopelliti, R. Tripier, H. Handel and A. E. Merbach, *Chem. Commun.*, 2002, 2630.
10 Z. Jászberényi, A. Sour, É. Tóth, M. Benmelouka and A. E. Merbach, *Dalton Trans.*, 2005, 2713.
11 (*a*) M. Woods, Z. Kovacs, S. Zhang and A. D. Sherry, *Angew. Chem., Int. Ed.*, 2003, **42**, 5889; (*b*) M. Woods, M. Botta, S. Avedano, J. Wang and A. D. Sherry, *Dalton Trans.*, 2005, 3829.
12 (*a*) P. Lebdušková, J. Kotek, P. Hermann, L. V. Elst, R. N. Muller, I. Lukeš and J. A. Peters, *Bioconjugate Chem.*, 2004, **15**, 881; (*b*) J. Kotek, P. Lebdušková, P. Hermann, L. Vander Elst, R. N. Muller, T. Maschmeyer, I. Lukeš and J. A. Peters, *Chem. Eur. J.*, 2003, **9**, 5899.
13 J. Rudovský, P. Cígler, J. Kotek, P. Hermann, P. Vojtíšek, I. Lukeš, J. A. Peters, L. V. Elst and R. N. Muller, *Chem. Eur. J.*, 2005, **11**, 2373.
14 (*a*) J. Rudovský, J. Kotek, P. Hermann, I. Lukeš, V. Mainero and S. Aime, *Org. Biomol. Chem.*, 2005, **3**, 112; (*b*) J. Kotek, J. Rudovský, P. Hermann and I. Lukeš, *Inorg. Chem.*, 2006, **45**, 3097.
15 M. Polášek, J. Rudovský, P. Hermann, I. Lukeš, L. V. Elst and R. N. Muller, *Chem. Commun.*, 2004, 2602.
16 M. Botta, *Eur. J. Inorg. Chem.*, 2000, 399.
17 J. Rudovský, P. Hermann, M. Botta, S. Aime and I. Lukeš, *Chem. Commun.*, 2005, 2390.
18 D. H. Powell, O. M. N. Dhubhghaill, D. Pubanz, L. Helm, Y. S. Lebedev, W. Schlaepfer and A. E. Merbach, *J. Am. Chem. Soc.*, 1996, **118**, 9333.
19 É. Tóth, S. Vauthey, D. Pubanz and A. E. Merbach, *Inorg. Chem.*, 1996, **35**, 3375.
20 E. Zitha-Bovens, L. Vander Elst, R. N. Muller, H. van Bekkum and J. A. Peters, *Eur. J. Inorg. Chem.*, 2001, 3101.
21 T.-M. Lee, T.-H. Cheng, M.-H. Ou, C. A. Chang, G.-C. Liu and Y.-M. Wang, *Magn. Reson. Chem.*, 2004, **42**, 329.
22 (*a*) W. H. Li, S. E. Fraser and T. J. Meade, *J. Am. Chem. Soc.*, 1999, **121**, 1413; (*b*) W. H. Li, G. Parigi, M. Fragai, C. Luchinat and T. J. Meade, *Inorg. Chem.*, 2002, **41**, 1418.
23 V. Comblin, D. Gilsoul, M. Hermann, V. Humblet, V. Jacques, M. Mesbahi, C. Sauvage and J. F. Desreux, *Coord. Chem. Rev.*, 1999, **186**, 451.
24 (*a*) R. Ruloff, G. van Koten and A. E. Merbach, *Chem. Commun.*, 2004, 842; (*b*) J. B. Livramento, É. Tóth, A. Sour, A. Borel, A. E. Merbach and R. Ruloff, *Angew. Chem., Int. Ed.*, 2005, **44**, 1480; (*c*) J. Costa, R. Ruloff, L. Burai, L. Helm and A. E. Merbach, *J. Am. Chem. Soc.*, 2005, **127**, 5147; (*d*) J. Costa, É. Tóth, L. Helm and A. E. Merbach, *Inorg. Chem.*, 2005, **44**, 4747; (*e*) J. B. Livramento, A. Sour, A. Borel, A. E. Merbach and É. Tóth, *Chem. Eur. J.*, 2006, **12**, 989.
25 S. Liu and D. S. Edwards, *Bioconjugate Chem.*, 2001, **12**, 7.
26 All lanthanide-containing NMR samples were tested for the presence of free lanthanide(III) by dropping the test solution into a urotropine buffered water solution of xylenol orange (pH 5). If the solution remained orange the test was negative.

27 M. C. Alpoin, A. M. Urbano, C. F. G. C. Geraldes and J. A. Peters, *J. Chem. Soc., Dalton Trans.*, 1992, 463.

28 For the DIS experiment, a series of complexes with variable concentrations of Dy^{3+} and 10% excess of the ligand was prepared.

29 (*a*) S. Aime, L. Barbero, M. Botta and G. Ermondi, *Inorg. Chem.*, 1992, **31**, 4291; (*b*) S. Hoeft and K. Roth, *Chem. Ber.*, 1993, **126**, 869.

30 (*a*) S. Aime, A. Barge, M. Botta, A. S. De Sousa and D. Parker, *Angew. Chem., Int. Ed.*, 1998, **37**, 2673; (*b*) M. Woods, S. Aime, M. Botta, J. A. K. Howard, J. M. Moloney, M. Navet, D. Parker, M. Port and O. Rousseaux, *J. Am. Chem. Soc.*, 2000, **122**, 9781; (*c*) F. A. Dunand, S. Aime and A. E. Merbach, *J. Am. Chem. Soc.*, 2000, **122**, 1506; (*d*) F. A. Dunand, R. S. Dickins, D. Parker and A. E. Merbach, *Chem. Eur. J.*, 2001, **7**, 5160; (*e*) S. Zhang, Z. Kovacs, S. Burgess, S. Aime, E. Terreno and A. D. Sherry, *Chem. Eur. J.*, 2001, **7**, 288.

31 (*a*) S. Aime, A. S. Batsanov, M. Botta, R. S. Dickins, S. Falkner, C. E. Foster, A. Harrison, J. A. K. Howard, J. M. Moloney, T. J. Norman, D. Parker and J. A. G. Williams, *J. Chem. Soc., Dalton Trans.*, 1997, 3623; (*b*) S. Aime, A. S. Batsanov, M. Botta, J. A. K. Howard, D. Parker, K. Senanayake and J. A. G. Williams, *Inorg. Chem.*, 1994, **33**, 4696.

32 W. D. Kim, G. E. Kiefer, J. Huskens and A. D. Sherry, *Inorg. Chem.*, 1997, **36**, 4128.

33 (*a*) J. Rohovec, P. Vojtíšek, P. Hermann, J. Mosinger, Z. Žák and I. Lukeš, *J. Chem. Soc., Dalton Trans.*, 1999, 3585; (*b*) J. Rohovec, P. Vojtíšek, I. Lukeš, P. Hermann and J. Ludvík, *J. Chem. Soc., Dalton Trans.*, 2000, 141.

34 S. Aime, M. Botta, M. Fasano, M. P. M. Marques, C. F. G. C. Geraldes, D. Pubanz and A. E. Merbach, *Inorg. Chem.*, 1997, **36**, 2059.

35 J. H. Freed, *J. Chem. Phys.*, 1978, **68**, 4034.

36 P. Vojtíšek, P. Cígler, J. Kotek, J. Rudovský, P. Hermann and I. Lukeš, *Inorg. Chem.*, 2005, **44**, 5591.

37 J. C. Hindman, *J. Chem. Phys.*, 1974, **60**, 4488.

38 (*a*) P. Caravan, M. T. Greenfield, X. Li and A. D. Sherry, *Inorg. Chem.*, 2001, **40**, 6580; (*b*) S. Aime, M. Botta, E. Terreno, P. L. Anelli and F. Uggeri, *Magn. Reson. Med.*, 1993, **30**, 583.

39 G. M. Nicolle, F. Yerly, D. Imbert, U. Böttger, J.-C. Bünzli and A. E. Merbach, *Chem. Eur. J.*, 2003, **9**, 5453.

40 É. Tóth, L. Helm and A. E. Merbach, in *The Chemistry of Contrast Agents in Medical Magnetic Resonance Imaging*, ed. A. E. Merbach and É. Tóth, Wiley, Chichester, UK, 2001, pp. 45–119.

41 J. A. Peters, J. Huskens and D. J. Raber, *Prog. Nucl. Magn. Reson. Spectrosc.*, 1996, **28**, 283.

42 In the ES/MS spectrum, there were many minor peaks corresponding to $(M + nNa)^-$ and $(M + nK)^-$ with a fine splitting due to the natural isotopic abundance of the gadolinium isotopes.

43 D. M. Corsi, C. Platas-Iglesias, H. van Bekkum and J. A. Peters, *Magn. Reson. Chem.*, 2001, **39**, 723.

44 *Scientist for Windows version 2.01*, Micromath Inc., Salt Lake City, UT, 1995.

45 *Origin version 6.0*, MicroCal Software Inc., Northampton, MA, 1999.

46 *HyperChem Release 7.5 for Windows, Molecular Modeling Systém*, Hypercube Inc., Ontario, Canada, 2002.

47 *MSI WebLabViewerPro 4.0* Preview, http://www.msi.com, 2000.